Opening of the Myosin Nucleotide Triphosphate Binding Domain during the ATPase Cycle†

Edward Pate,*,‡ Nariman Naber,§ Marija Matuska,§ Kathleen Franks-Skiba,§ and Roger Cooke§

Department of Pure and Applied Mathematics, Washington State University, Pullman, Washington 99164, and Department of Biochemistry and Biophysics and Cardiovascular Research Institute, University of California, San Francisco, California 94143

Received April 29, 1997; Revised Manuscript Received June 24, 1997⊗

ABSTRACT: A series of ATP analogs, in which moieties of various sizes have been added to the γ-phosphorus of ATP, bind to the active site of myosin and to the actomyosin complex in myofibrils and in chemically skinned fibers. The affinity of the analogs for the active site shows only a slight dependence on the size of the added moiety. Addition of even our smallest group (CH_3) reduced the binding affinity of ATPγ-CH_3 for S1 to 40 μM, a factor of 10^5 less than observed for ATP. Computer molecular docking of ATP-γCH_3 into the myosin−ADP·BeF_3 crystal structure of *Dictyostelium discoideum* indicates no steric interference to prevent binding. This suggests that the maintenance of charge at the γ-phosphate is crucial for tight nucleotide binding. Addition of larger groups, (1) an EPR probe (ATP-γSL) or (2) ADP (i.e., P^1,P^5-diadenosine pentaphosphate, AP_5A), reduced the affinity by only approximately a factor of 10 over that of ATP-γCH_3. In the crystal structure of S1 complexed with nucleotides, the phosphates are buried within a protein structure called "the phosphate tube". Both the bulk of the modifying groups and the lack of dependence on the size of the group are incompatible with threading of the phosphates down the P_i-tube, showing that the tube must open. Similar domain movements have been found in other proteins including members of the G-protein superfamily, a family that has structural homologies to myosin.

A primary goal among muscle physiologists is to understand how the structural constraints inherent in both the myosin molecule and the substrate, ATP, interact to produce the protein conformational changes necessary for force and motion in biological systems. This quest has received renewed impetus from several recent X-ray crystallographic protein structures. Rayment and colleagues have provided high-resolution structures of the nucleotide-bound motor domain of *Dictyostelium discoideum* (*Dd*)[1] myosin and nucleotide-free S1 from chicken (*1*−*3*). Fletterick, Kull, Sablin, and colleagues (*4*, *5*) have recently solved the structures of the microtubule-based motors, kinesin and ncd. The unanticipated, but ineluctable, structural similarities between myosin, kinesin, ncd, and previously determined X-ray structures for members of the guanyl nucleotide-binding protein family have been taken to suggest that all of these proteins, which serve disparate functions within the cell, belong to a superfamily deriving from a common ancestor (*4*, *6*). Irrespective of whether convergent or divergent evolution be the path to the common structural motifs among these proteins, structure−function relationships deduced from the investigation of one family of proteins may now be anticipated to shed light on structure−function relationships in the other families. This latter observation motivates the experiments reported here.

In the X-ray structure of nucleotide-bound *Dd* myosin, the nucleotide binding pocket is in a relatively open conformation in the region surrounding the adenine and ribose groups (*2*, *3*). The triphosphates, on the other hand, are tightly encased in a narrow tubelike structure with the vector from the α- to the γ-phosphate pointing away from the open adenosine portion of the pocket. At the γ-phosphate end of this "phosphate tube" is an opening into the large cleft separating the upper and lower 50K myosin domains. This cleft constitutes a fairly large gap in the S1 molecule; indeed, looking up the cleft from the actin binding domain toward the P_i-tube, the occupancy of the γ-phosphate position is clearly visible in the myosin−ADP·BeF_3 crystal structure of *Dd* myosin (*2*, *7*).

Both the fundamental topologies and substantial amino acid sequence homologies are conserved when the P_i-tube portion of myosin is compared to the motor proteins, kinesin and ncd, as well as members of the G-protein family. The P_i-tube is composed of the Walker A, P-loop, sequence (*8*) common to many nucleotide binding proteins (amino acid sequence Gx_4GKT/S in the motor proteins, amino acids 179−186 in *Dd* myosin, GxxGxGKT/S in the G-proteins), switch I (amino acid sequence NxxSSR in the motor proteins, amino acids 233−238 in *Dd* myosin, Dx_nT in the G-proteins), and switch II (amino acid sequence DxxGxE in the motor proteins, amino acids 454−459 in *Dd* myosin, DxxG in the G-proteins) (*9*). Here we are using the "switch" notation more commonly found in the G-protein literature to identify the relevant portions of the proteins.

† This work was supported by USPHS Grants AR39643 (E.P.) and HL 32145 and AR42895 (R.C.).

* Corresponding author. Tel: 509-335-3151. FAX: 509-335-1188. E-mail: epate@wsu.edu.

‡ Washington State University.

§ University of California, San Francisco.

⊗ Abstract published in *Advance ACS Abstracts,* September 1, 1997.

[1] Abbreviations: AMPPNP, β,γ-imidoadenosine 5′-triphosphate; AP_5A, P^1,P^5-diadenosine pentaphosphate; ATP-γSL, P^3-(1-oxy-2,2,5,5-tetramethyl-3-pyrrolin-3-yl)methyl P^1-5′-adenosine triphosphate; ATP-γCH_3, P^3-methyl P^1-5′-adenosine triphosphate; caged ATP, P^3-[1-(2-nitrophenyl)ethyl]adenosine 5′-triphosphate; *Dd*, *Dictyostelium discoideum*; ϵATP and ϵADP, 1-N^6-ethenoadenosine triphosphate and diphosphate, respectively; MOPS, 3-(*N*-morpholino)propanesulfonic acid; pPDM, *N*,*N*′-*p*-phenylenedimaleimide; PP_i, inorganic pyrophosphate; S1, myosin subfragment 1.

S0006-2960(97)00996-3 CCC: $14.00

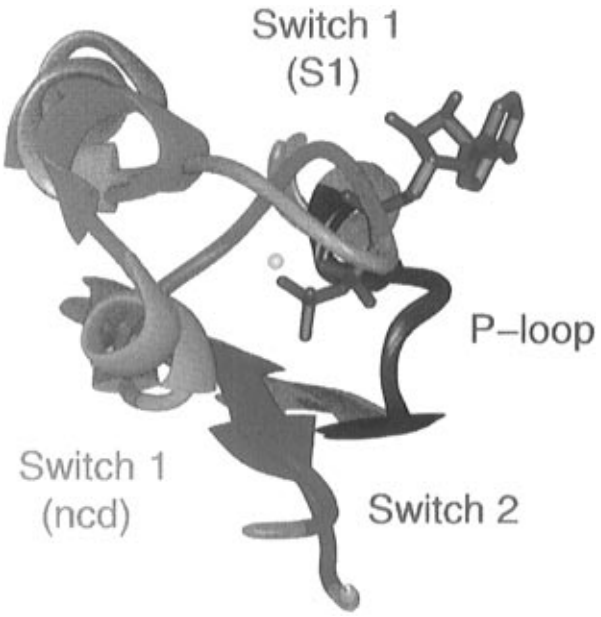

FIGURE 1: Ribbon diagram overlays of the *Dd* S1·ADP·BeF_3 and the ncd crystal structures in the region of the ligand triphosphate domain. S1 is shown in gray and ncd in cyan, with the following exceptions: the conserved sequences (see text) in the P-loops are colored dark blue and those for the switch II domain are colored magenta for both structures; the conserved sequence in the switch I domain for S1 is shown in green; that for ncd is shown in gold. The bound nucleotide from the *Dd* S1·ADP·BeF_3 structure is shown in red; the metal, in yellow. The bound ligand (ADP) in the ncd structure (*5*) is very close to the location of the ADP portion of the ligand in the X-ray crystallographic *Dd* S1·ADP·BeF_3 structure and is omitted for clarity. The important observation is that, in the S1 structure, the switch I region is a loop that overlays the ligand and, along with the P-loop and switch I, forms a closed "P_i-tube". In ncd, the switch II region has pulled back in a loop−α-helix motif (gold), and the ligand is now accessible to solvent. In kinesin, the gold, switch I domain is pulled back an additional 1−1.5 Å, forming an even more open nucleotide binding domain (not shown).

Despite the above similarities among the diverse proteins, an important difference at the active site triphosphates can be observed when the available X-ray crystallographic structures are superimposed. We shall use the structures of *Dd* myosin (*2*), the G-protein α-subunit, $G_{i\alpha1}$ (*10*), elongation factor Tu (EF-Tu) (*11*), human kinesin (*4*), and *Drosophila* ncd (*5*) as representative cases. Overlaying all five proteins shows that the P-loop and switch II portions of the P_i-tube are at virtually superimposable spatial locations with respect to the triphosphates in all cases. Just as found in the myosin motor domain, a space-filling model of the G-protein α-subunit, $G_{i\alpha1}$, shows that the switch I portion of the protein also contributes to a tightly closed P_i-tube. EF-Tu, on the other hand, has a P_i-tube that is more open, with limited solvent accessibility to the triphosphates now possible along the length of the tube. This is in part due to a displacement of a portion of the switch I amino acid backbone away from the triphosphates. At the extreme, the X-ray crystal structures of kinesin and ncd show that switch I is pulled away from the ligand, being located quite far from switch II, the P-loop, and the phosphates. Indeed, due to the magnitude of the switch I displacement in the ncd and kinesin structures, the phosphates are not enclosed in a tube structure. This topology is demonstrated in an overlay of S1 and ncd in Figure 1. The nucleotide binding domain in S1 has been replaced in ncd by a structure that more closely resembles an open trough in which the phosphates of the ncd ligand (ADP) are exposed to solvent.

Accepting that the sequence and topological similarities between the proteins enhance the possibility of common protein domain movements during their hydrolytic cycles, and viewing the succession of X-ray structures as functioning as "snapshots in time" of such a conformational change, it becomes legitimate to ask whether myosin undergoes large-scale movements which open the P_i-tube during the contractile cycle? To address this question, we have investigated the affinity of a series of ATP analogs for S1 and the conformational changes induced in S1 by their binding, as well as their mechanical perturbations in skinned muscle fibers. The analogs contain moieties of various sizes connected by a phosphate ester linkage to the γ-phosphorus of ATP. Previous work has shown that "caged ATP" can bind to the myosin nucleotide site in muscle fibers (*12*, *13*). This analog has a moderately sized, substituted phenyl ring on the γ-phosphate. Here we have investigated analogs with a series of moieties of differing sizes, some very large. All analogs bound to S1 and affected skinned fiber mechanics, but to various degrees. Computer molecular docking studies were then performed to determine the implications for structural changes during the ATPase cycle, and we conclude that the P_i-tube must open during the ATPase cycle.

METHODS

Syntheses

*P^3-Methyl P^1-5′-Adenosine Triphosphate (Compound **1**).* Adenosine 5′-triphosphate was converted to the γ-methyl ester following the procedure of Eckstein et al. (*14*).

*P^3-(1-Oxy-2,2,5,5-tetramethyl-3-pyrrolin-3-yl)methyl P^1-5′-Adenosine Triphosphate (Compound **2**).* 1-Oxy-3-(hydroxymethyl)-2,2,5,5-tetramethyl-3-pyrroline was synthesized following the method of Hideg et al. (*15*). It was then reacted with adenosine triphosphate to give the γ-spin-labeled ester of ATP (compound **2**) following the same procedure for the synthesis of the γ-methyl ester (*14*). Thin-layer chromatography was run on silica gel using 1-propanol/ammonia/water, 6/3/1, with 0.5 g/L EDTA: R_f 0.24.

Mass spectroscopy was done using a Sciex API 300 mass spectrometer with the negative ion mode using 1/1 methanol/H_2O. MS: 658 (M − H), 680 (M^+ − Na). The structures of ATP-γCH_3, ATP-γSL, and AP_5A are shown in Figure 2.

Fluorescence Nucleotide Analog Binding Studies

Myosin S1 was prepared from rabbit fast skeletal muscles following the method of Margossian and Lowey (*16*). Myofibrils were prepared as described in Franks-Skiba et al. (*17*). Nucleotide analog affinities for S1 and myofibrilar actomyosin were determined by binding competition experiments with fluorescent ϵADP. The experimental buffer contained 10 mM $MgCl_2$, 20 mM MOPS, 1 mM EGTA, 25 μM S1 or 15−20 mg/mL myofibrils, 0.02 mg/mL apyrase, 22−40 μM ϵADP, and 400 mM acrylamide, pH 7.0, 20 ± 0.5 °C, with additions as noted. ϵADP was initially added in the triphosphate form. Under comparable conditions, the ϵATPase rate was >0.2 s^{-1} (*17*−*19*), and thus the ϵATP was rapidly hydrolyzed to the diphosphate form. Previous studies (*17*, *20*, *21*) have shown that ϵADP was almost

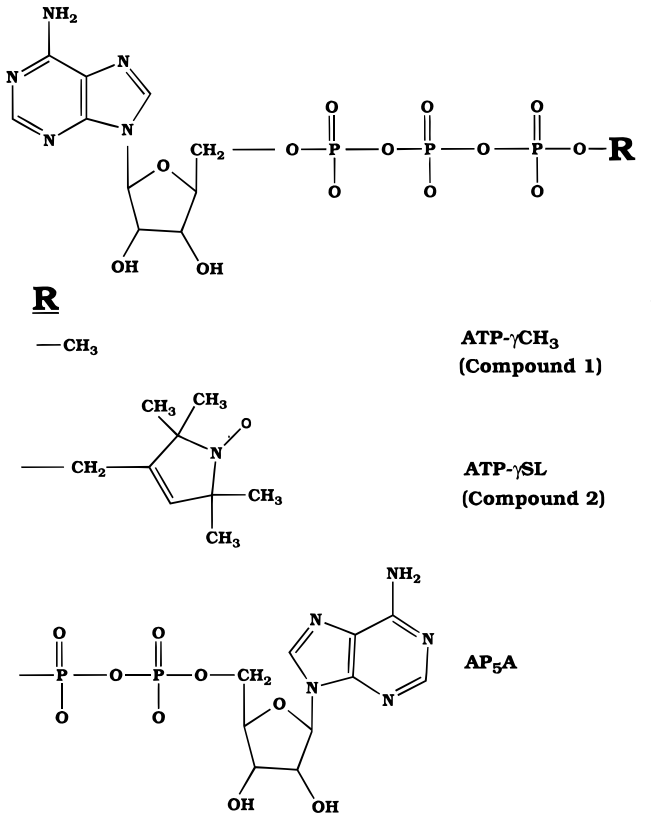

FIGURE 2: Structures of the analogs used in the binding studies.

completely protected from solvent acrylamide quenching when bound to the active site of S1 or myofibrilar actomyosin. Nucleotide analog binding was determined from the change in fluorescence in binding competition experiments between the fluorescent nucleotide and the nucleotide analog. Fluorescence was collected using the front-face optical path from a 2 mm thick cell in the temperature-controlled fluorometer previously described (*17*), with $\lambda_{exc} = 320$ nm, $\lambda_{obs} = 410$ nm, and excitation and emission slit widths of 2.5 mm. Front-face fluorescence was used due to the turbidity of the solutions. At the concentrations of fluorescent nucleotides used in these studies, the optical density of the sample was less than 0.1. This is too small to influence our results. The fluorescence signal from bound fluorescent nucleotide was initially observed in the absence of added analog (see Figure 3). Following addition of a nucleotide analog, the decrease in steady-state fluorescence was determined. The fluorescence intensity following the subsequent addition of 0.25 mM ATP was taken as a baseline representing no bound fluorescent nucleotide. This contribution to the fluorescence signal was subtracted out in determining the dissociation constant. After further adjustment for buffer volume dilution factors, the total proportional decrease in fluorescence intensity for a given concentration of a nucleotide analog was used to determine an affinity constant for S1 or actomyosin as follows.

Let K_F and K_A be the dissociation constants of the fluorescent nucleotide and the nucleotide analog, respectively, to S1 (or actomyosin). To simplify notation, let S, A, and F represent S1, the nucleotide analog, and the fluorescent analog, respectively, with S_{ai}, A_{ai}, and F_{ai} representing the concentrations of S1, analog, and fluorescent analog that have been added in the $i \in [1,n]$ repetition of the fluorescence competition experiment for a given ATP analog. Then from mass action

$$\begin{aligned} K_F[F{\cdot}S]_i - [F]_i[S]_i &= 0 \\ [F{\cdot}S]_i + [F]_i &= F_{ai} \\ K_A[A{\cdot}S]_i - [A]_i[S]_i &= 0 \\ [A{\cdot}S]_i + [A]_i &= A_{ai} \\ [A{\cdot}S]_i + [F{\cdot}S]_i + [S]_i &= S_{ai} \end{aligned} \tag{1}$$

For given binding constants and known concentrations, S_{ai}, A_{ai}, and F_{ai}, this nonlinear system of equations can be solved to yield the five unknown concentrations, $[F{\cdot}S]_i$, $[F]_i$, $[S]_i$, $[A{\cdot}S]_i$, and $[A]_i$. K_F has previously been determined under conditions identical to those used here (*17*). K_A is the parameter we wish to determine from our fluorescence observations. Let $I_i(0)$ represent the observed fluorescence signal in the absence of added nucleotide analog, i.e., $A_{ai} = 0$, corresponding to a known concentration of fluorescent nucleotide bound S1 of $[F{\cdot}S]_{0i}$ since K_F is known. Here the first subscript signifies the absence of added nucleotide analog, the second signifies the *i*th experimental repetition. Let $I_i(A_{ai})$ be the observed fluorescence signal upon addition of nucleotide analog concentration, A_{ai}, and let I_i(ATP) represent the observed fluorescence signal after addition of 0.25 mM ATP at the conclusion of the experiment (zero bound fluorescent analog). By linear interpolation, the *experimentally observed* concentration of fluorescent nucleotide-bound S1 for added concentration A_i is taken to be

$$[F{\cdot}S]_{obs\ i} = [F{\cdot}S]_{0i}\{I_i(A_i) - I_i(\text{ATP})\}/\{I_i(0) - I_i(\text{ATP})\}$$

Similarly, for a given K_A and known additions, eq 1 can be solved to determine a *calculated* concentration of fluorescent nucleotide-bound S1, $[F{\cdot}S]_{calc\ i}$. Then our desired approximation to the dissociation constant, K_A, is taken as that value which minimizes the sum of squared differences, $\chi^2(K_A)$, over all observations between the observed and calculated concentrations of F·S, i.e., the K_A minimizing

$$\chi^2(K_A) = \sum_{i=1}^{i=n}([F{\cdot}S]_{obs\ i} - [F{\cdot}S]_{calc\ i})^2 \tag{2}$$

At each step, the nonlinear eq 1 was solved using a Newton iteration technique. The minimization on K_A (eq 2) was accomplished using the Harwell library subroutine, VA04A. The dissociation constant, K_F, of ϵADP to S1 was taken to be 11 μM; the dissociation constant of ϵADP to myofibrilar actomyosin was taken to be 50 μM (*17*). Additional details are provided in Results.

Previous studies with ligands that bind weakly to S1 and actomyosin have shown the importance of adapting protocols that eliminate the possibility of inadvertent ATP and ADP contamination (*22*). All synthesized ligands and purchased P^1,P^5-diadenosine pentaphosphate (AP_5A, Boeringer) were purified by HPLC. Apyrase (potato, grade V, Sigma Chemical Co.) was also then included in experimental buffers to the extent possible. At a 1 mg/mL apyrase concentration, thin-layer chromatography revealed no detectable hydrolysis of AP_5A, ATP-γSL, or ADP-γCH_3 (5 mM) over a period of 1 h at 20 °C. However, ϵATP and ϵADP did prove to be very poor substrates for apyrase. Thus, for experiments

involving these fluorescent analogs, buffer concentrations of apyrase were kept below 0.02 mg/mL. At this level, no statistically significant decrease in fluorescence could be detected due to the presence of apyrase over the ≤200 s time course of the fluorescence experiments (see Figure 3). For experiments involving AP_5A, ATP-γCH_3, and ATP-γSL, additional precautions were taken. Initial stock solutions (30 mM) included 1 mg/mL apyrase, 5 mM $MgCl_2$, and 20 mM MOPS, pH 7.0, and were allowed to sit at room temperature for 1 h. In some stock solutions, 5 mg/mL myofibrils were also added. The solutions were then filtered via centrifugation through a 10 kDa cutoff filter, divided into aliquots, and stored at −20 °C until immediately prior to use. The molecular mass of potato apyrase is ≥40 kDa (*23*). Analytical HPLC was also used to evaluate analog purity. For fluorescence experiments, apyrase was then readded, subject to the 0.02 mg/mL constraint discussed above.

Protein concentrations were determined by the method of Bradford (*24*). The molecular mass of S1 was taken as 120 kDa, the molecular mass of monomeric myosin was taken as 230 kDa, and 45% of the myofibrilar protein was assumed to be myosin (*25*). ϵATP was obtained from Molecular Probes. Acrylamide was obtained from Bio-Rad.

Changes in tryptophan fluorescence associated with ligand binding were monitored using a buffer containing 10 mM $MgCl_2$, 20 mM MOPS, 1 mM EGTA, 10 μM S1, and 0.02 mg/mL apyrase, pH 7.0, 20 ± 0.5 °C, with additions as noted. Fluorescence changes were monitored following addition of a nucleotide or nucleotide analog (0.5 mM ATP, ADP, or ATP-γCH_3; 2 mM ATP-γSL or AP_5A) using the previously described (*17*) fluorometer setup with λ_{exc} = 297 nm, λ_{obs} = 340 nm, and excitation and emission slit widths of 0.5 mm. For observations of the change in fluorescence solely in the presence of ATP or ADP, apyrase was omitted from the buffers. In other experiments, the enhancement of fluorescence by ATP was determined by adding 0.25 mM ATP subsequent to addition of either ATP-γCH_3, ATP-γSL, or AP_5A (see Figure 5). No significant difference in the ATP-induced enhancement was observed when compared to experiments in which ATP was added alone, and the data were combined for statistical analysis. Additional controls in the absence of S1 showed that none of the ligands resulted in any statistically significant change in the fluorescence signal via binding to the 0.02 mg/mL apyrase. Addition of 250 μM AP_5A to 25 μM myokinase (Sigma Chemical Co.) resulted in no change in the fluorescence signal, allowing us to rule out the possibility of trace myokinase contamination in our S1 preparation influencing our results.

pPDM Cross-Linking of SH-1 and SH-2

For reactive sulfhydryl cross-linking studies, S1 was dialyzed into a buffer containing 50 mM Tris, 100 mM KCl, and 0.2 mM phenylmethanesulfonyl fluoride (PMSF), pH 8.0, 0 °C. All subsequent steps were done at 20 °C. S1 (20 μM) was incubated for 10 min in the presence of 2 mM additional $MgCl_2$ and 40 μM ligand. The cross-linking reaction was initiated by addition of 25 μM *N,N′-p*-phenylenedimaleimide (pPDM). In control experiments, pPDM and/or ligand were (was) omitted. After variable times (5, 25, 50 min), 200 μM 2-mercaptoethanol was added and the cross-linking reaction was quenched on ice. pPDM was obtained from Aldrich and crystallized in dichloromethane. The purified pPDM crystals were yellow in color. A 1 mM stock solution was made in acetonitrile and kept frozen until use (*26*). The extent of cross-linking was monitored via the S1 Ca^{2+}-ATPase in a buffer containing 0.6 M KCl, 50 mM MOPS, and 4 mM $CaCl_2$, pH 7.0, 20 °C. The ATPase reaction was initiated by addition of 1 mM ATP. Five aliquots were taken at 1 min intervals, and the liberated phosphate was determined using the malachite green assay (*27*). A least-squares, linear fit to the phosphate data was used to determine the ATPase rate.

Muscle Fiber Mechanics

Rabbit psoas fibers were harvested and chemically skinned as described previously (*28*). For mechanical experiments, single fibers were dissected from a bundle of fibers and mounted in a well between a solid-state force transducer and a rapid motor for changing fiber length. Fiber mounting and the experimental apparatus have been described in detail elsewhere (*28*, *29*). The "temperature jump" protocols of Pate et al. (*30*) were employed for determining fiber shortening velocity. The fiber was initially immersed in a solution containing 12 mM $Mg(OAc)_2$, 40 mM MOPS, 1 mM EGTA, 1.1 mM $CaCl_2$, 0.09 M KOAc, 20 mM phosphocreatine, 2 mg/mL creatine phosphokinase, and variable amounts of substrate and nucleotide analog, pH 7.0, 2 °C. The fiber was then rapidly (<2 s) transferred to an identical buffer, except at pH 7.0, 20 °C. We have previously shown that this yields stable isotonic contractions for skinned rabbit skeletal muscle fibers at temperatures exceeding the 20 °C temperature of the present experiments (*30*).

Following transfer to the higher temperature buffer, the fiber was then allowed to shorten isotonically at 5% of P_o ($V_{0.05}$). This value at a low shortening tension was used as an approximation to the maximum shortening velocity. Linear, double reciprocal plots of $1/V_{0.05}$ vs 1/[MgATP] were used to approximate the value of the inhibition constant, K_i, of the ligand being studied, assuming classical, Michaelis−Menten saturation behavior. Control experiments in the absence of added ligand were done to determine the Michaelis constant, K_m, for shortening velocity at 5% P_o with MgATP as substrate.

Computer Molecular Docking

All molecular modeling was done on a Silicon Graphics Indigo R4400 workstation using Insight (Ver 95.0, Biosym). The coordinates for the "ATP portion" of the synthesized analogs were taken as the coordinates of ADP·BeF_3 from the X-ray structure of the *Dd* S1 complex (*2*). AP_5A was then modeled by joining the ADP coordinates from the same crystal structure, assuming a P-O-P bond angle of 135° and a P−O bond length of 1.56 Å. ATP-γCH_3, ATP-γSL, and caged ATP were similarly constructed by starting with the ADP·BeF_3 coordinates. The docking was then done with the ATP portion fixed with respect to the protein as in the crystal structure, allowing rotations only about single bonds in the esterified moiety. Rotations were also allowed in the side chains of amino acids located at the end of the P_i-tube and the upper portion of the 50 K cleft. No backbone modifications were allowed. A 1 Å van der Waals radius was assumed in defining the van der Waals surface. Steric interference was assumed to be present if there was spatial

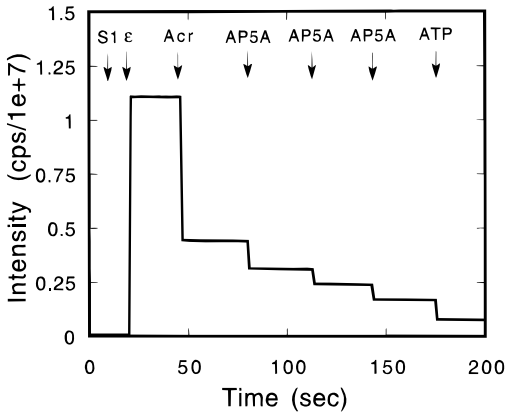

FIGURE 3: Fluorescence intensity as a function of time for the determination of the binding constant of AP_5A to S1. Additions are denoted by arrows. Arrow S1 gives the background fluorescence when only buffer containing 25 μM S1 is added to the fluorometer cuvette. Arrow ϵ indicates addition of 22 μM ϵADP, with a concomitant increase in the fluorescence signal. At arrow Acr, 400 mM acrylamide is added, quenching the fluorescence signal from ϵADP that is not bound to S1. At arrows AP_5A, sequential additions bring the total added AP_5A to approximately 0.5, 1, and 2 mM, respectively, and decrease the observed fluorescence signal as AP_5A displaces bound, protected ϵADP from the active site into solution where its fluorescence is quenched. Prior to each addition, the fluorometer shutter was closed and data collection was paused. ϵATP or ligand was added, and the cuvette was allowed to sit for 60−90 s. This was to ensure that the ϵATP was hydrolyzed to ϵADP and that the apyrase was allowed sufficient time to hydrolyze any residual contaminating ATP or ADP in the added ligand. Data collection was then started anew. At arrow ATP, 0.25 mM ATP is added, establishing a baseline representing zero bound AP_5A. Note that, after each addition, fluorescence is constant as a function of time. Thus the presence of 0.02 mg/mL apyrase in the experimental buffers does not result in a decrease in fluorescence with time as would occur if any significant degradation of the ϵADP to ϵAMP were occurring.

overlap between the surfaces around the ligand and the protein (including side chains). Additional details are provided in the Discussion.

RESULTS

We have employed four different techniques to probe the binding of γ-phosphate modified nucleotide analogs to S1 and to actomyosin: (1) competition with a fluorescent substrate, (2) enhancement of intrinsic tryptophan fluorescence, (3) enhancement of pPDM sulfhydryl cross-linking, and (4) skinned muscle fiber mechanics.

(1) Competition with a Fluorescent Substrate. The ability of the series of analogs to bind to the active site of myosin was determined by competition with ϵADP. Representative data are shown in Figure 3 with AP_5A as the competing species. S1 was incubated with 25 μM ϵADP and a 400 mM portion of the collisional quencher, acrylamide. As shown by previous workers, the fluorescence of ϵADP bound to the active site of S1 is protected from quenching by the acrylamide, while the fluorescence of the free nucleotide is readily quenched. Addition of an analog that binds to the active site will displace a fraction of the bound ϵADP, resulting in the sequential decreases in fluorescence observed in Figure 3 (arrows marked AP_5A). Addition of ATP at the end of the experiment establishes a baseline representing zero bound analog. Figure 4a shows the accumulated relative fluorescence data for ATP-γCH_3 (diamonds), ATP-γSL (squares), and AP_5A (circles) from competition experiments involving S1. Figure 4b gives the corresponding data from competition experiments for actomyosin in myofibrils. The dissociation constants were determined from the least-squares fits, also shown in Figure 4, as described in Methods (eqs 1 and 2). The values obtained are summarized in Table 1. Literature values for the physiological species, ATP and ADP, and caged ATP are likewise included in Table 1 for comparison.

Table 1: Biochemical Parameters for the Analogs Studied Using S1 and Myofibrilar Actomyosin (A·M)[a]

analog	K_d (S1)	K_d (A·M)	K_i (fiber vel)	fluorescence enhancement (%)
ATP-γCH_3	42 ± 2.7 μM	801 ± 51 μM	1.2 mM	12.2 ± 0.9(16)
ATP-γSL	565 ± 14 μM	3.02 ± 0.19 mM	13 mM	9.3 ± 0.7 (4)
AP_5A	251 ± 6.6 μM	1.52 ± 0.08 mM	1.8 mM	7.1 ± 0.4 (9)
caged ATP	350 μM[b]	1.6 mM[b]	1−2 mM[c]	
ATP	0.1 nM[d]	1 μM[e]		25.7 ± 1.1(16)
ADP	1−5 μM[f]	150 μM[f]	250 μM[g]	10.8 ± 0.5 (5)

[a] Dissociation constants, K_d, were determined by a least-squares approach (see Methods) from data in Figure 3. The inhibition constant, K_i, was determined from skinned fiber velocity. Values were determined from least-squares, double reciprocal plots as in Figure 5. The increase in S1 tryptophan fluorescence in the presence of added ligand was monitored at 0.5 mM ligand concentration, with the exception of ATP-γSL and AP_5A. For these ligands the concentration was raised to 2 mM. The initial S1 concentration was 10 μM for all fluorescence experiments. For comparison, literature values are given for the physiological species, ATP and ADP, and caged ATP. See footnotes *b*−*g*. [b] Based upon single-turnover, competition experiments with ATP (*12*). [c] Thirlwell et al. (*13*). [d] Reviewed by Taylor (*42*). [e] Estimated by Sleep and Smith (*44*). [f] Greene and Eisenberg (*43*). [g] Cooke and Pate (*38*).

(2) Enhancement of Tryptophan Fluorescence. The binding of ATP to S1 results in a conformational change in the protein that can be monitored by changes in the tryptophan fluorescence. This effect was measured and showed that the analogs studied here bound to the active site and produced changes in the protein structure, but to various degrees and to a lesser extent than produced by ATP. Binding of nucleotides is known to alter the fluorescence of Trp-510 in chicken myosin (*31*). This location is distant from the active site, near the junction of the catalytic domain and the light chain domain. This residue is conserved across a wide range of myosins, including the rabbit skeletal protein used in the present studies (*32*). Data from an experiment monitoring changes in tryptophan fluorescence with AP_5A and ATP as ligands are shown in Figure 5. Mean increases in tryptophan fluorescence observed as a function of ligand are summarized in Table 1. Controls with ATP resulted in an increase in tryptophan fluorescence of approximately 25%, and with ADP an increase of approximately 10% was observed. Similar values have been reported previously (*33*). We found that all of the other ligands enhanced tryptophan fluorescence, although to various degrees. ATP-γCH_3 resulted in the largest increase (12% ± 1%) and AP_5A the least (7% ± 0.4%). Nonetheless, the data strengthen our conclusion that the ligands are binding to the nucleotide site of S1 and show in addition that they promote conformational changes at a distant site in a manner similar to the physiological nucleotides.

(3) pPDM Cross-Linking of the Reactive Sulfhydryls. Previous studies have shown that the presence of bound nucleotide enhances the susceptibility of the reactive myosin

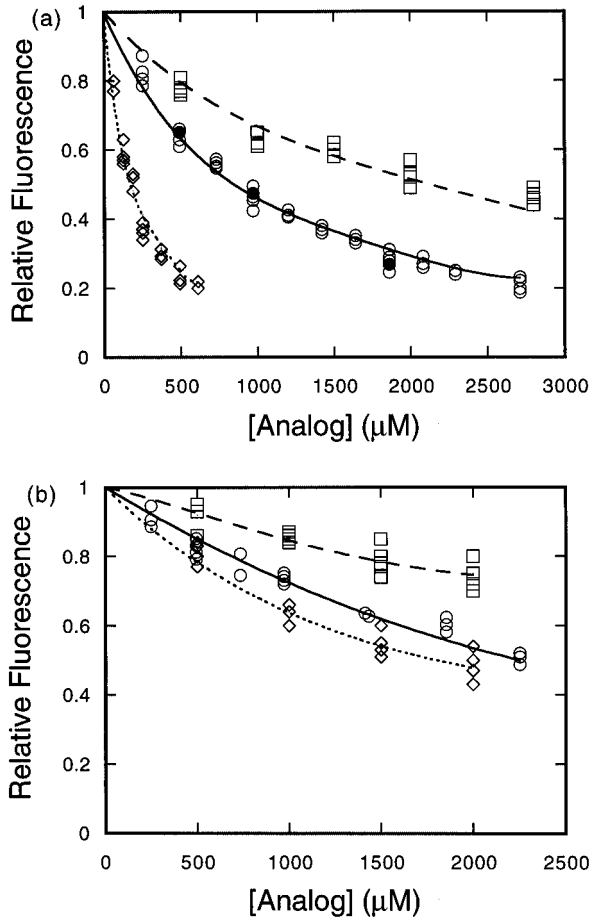

FIGURE 4: Fluorescence signal normalized with respect to volume dilutions and baselines as described in the text from (a) S1 and from (b) myofibrilar, actomyosin fluorescence quenching competition experiments involving ATP-γCH$_3$ (diamonds), ATP-γSL (squares), and AP$_5$A (circles). In (a), the initial concentrations of S1 and ϵATP were 25 and 22 μM, respectively. The solid circles are the AP$_5$A data from Figure 2. In (b), the initial concentrations of myosin heads (ϵATP) were 44 μM (40 μM), 46 μM (40 μM), and 36 μM (25 μM) for ATP-γCH$_3$, AP$_5$A, and ATP-γSL, respectively. The least-squares fits to determine the binding constant as described in Methods are also shown.

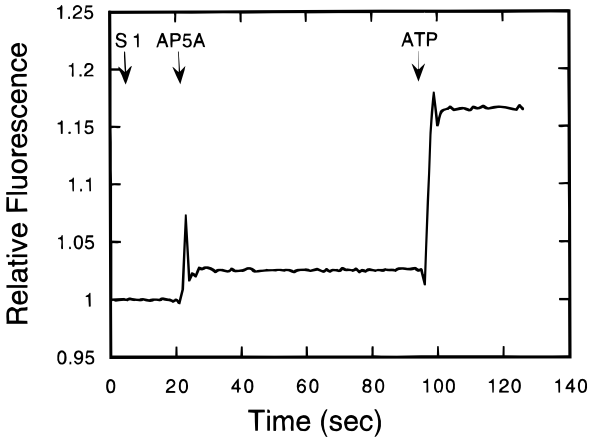

FIGURE 5: Change in tryptophan fluorescence for AP$_5$A binding to S1 as a function of time. The initial S1 concentration was 10 μM. Arrow S1 denotes only S1 in the fluorometer cuvette. At arrow AP$_5$A, 2 mM AP$_5$A was added to the fluorometer cuvette, and the observed fluorescence increased. At arrow ATP, an additional 0.5 mM ATP was added. After being adjusted for volume dilutions (5.2% for AP$_5$A, 1.2% for ATP), the data in Figure 4 define a fluorescence increase in this experiment of 7.6% for AP$_5$A and 23.9% with ATP. The mean fluorescence increases as a function of nucleotide from repetitions of the experiment are summarized in Table 1. The values obtained in Figure 4 are within the experimental scatter of Table 1. The deviations at the second and third arrows in the fluorescence vs time plot in Figure 4 are artifacts resulting from opening the cuvette chamber and stirring the experimental solution following the additions of ligands.

Table 2: Relative Ca^{2+}-ATPase of pPDM Cross-Linked S1 as a Function of Nucleotide[a]

	Ca^{2+}-ATPase (% control) (unmodified S1 = 100%)		
conditions	5 min	25 min	50 min
no nucleotide	NM	124 ± 7 (6)	106 ± 11 (3)
ADP	31 ± 3 (2)	33 ± 4 (6)	29 ± 5 (3)
ATP-γCH$_3$	27 ± 3 (3)	27 ± 4 (4)	NM
ATP-γSL	101 ± 3 (3)	99 ± 8 (3)	87 ± 6 (2)
AP$_5$A	115 ± 2 (3)	62 ± 5 (6)	42 ± 5 (3)

[a] The cross-linking reaction was quenched at 5, 25, and 50 min. Data are given as mean ± SEM (number of observations). 100% corresponds to a control, unmodified S1, Ca^{2+}-ATPase of 1.14 ± 0.02 (5) P_i S1^{-1} s^{-1}. NM = not measured.

sulfhydryls, SH-1 and SH-2, for irreversible cross-linking by pPDM. The Ca^{2+}-ATPase activity can then be used to monitor the extent of cross-linking (reviewed in ref *26*). We thus examined the ability of our series of ligands to promote sulfhydryl cross-linking. Results are summarized in Table 2. In the presence of pPDM, but in the absence of ligand, Ca^{2+}-ATPase was elevated after even 50 min of cross-linking. In the presence of pPDM and ADP, we observed an ~70% decrease in the Ca^{2+}-ATPase when compared to unmodified S1. Increases and decreases in the Ca^{2+}-ATPase in the absence and presence of added ligand, respectively, have been previously reported (*34*, *35*). Ca^{2+}-ATPase values obtained from pPDM cross-linking in the presence of ATP-γCH$_3$, ATP-γSL, and AP$_5$A using 5, 20, and 50 min time courses are also given in Table 2. The ATPase observations for all ligands indicated that pPDM cross-linking was enhanced by the ATP analogs. The time courses and magnitudes observed were clearly different, however. In the presence of ADP and ATP-γCH$_3$, the cross-linking reaction had basically gone to completion in only 5 min and produced the largest decreases in the Ca^{2+}-ATPase. In contrast, AP$_5$A and ATP-γSL produced decreases that were still changing after 50 min. However, the rate of cross-linking was clearly greater than control. Thus, although the reaction is slower, pPDM cross-linking of the myosin reactive sulfhydryls is clearly enhanced by the presence of ATP-γCH$_3$, AP$_5$A, and ATP-γSL.

The data of Table 2 show that the presence of AP$_5$A and ATP-γSL promotes sulfhydryl cross-linking but not as effectively as does ADP. However, the rate of cross-linking should depend strongly on the fraction of S1 with bound ligand. For AP$_5$A and ATP-γSL, this fraction is lower than with ADP. For the conditions under which the AP$_5$A experiments were done (20 μM S1, 40 μM ligand), the 250 μM dissociation constant of AP$_5$A to S1 (Table 1) implies that, at the initial equilibrium, only about 10% of the S1 is complexed to AP$_5$A. The 1−5 μM binding constant of ADP to S1 implies that 80−95% of the S1 is complexed to ADP. Thus AP$_5$A would be expected to promote cross-linking at a rate 8−10 times more slowly than ADP due to the much weaker binding of AP$_5$A. With ATP-γSL and a K_d of 560 μM, the initial bound fraction of S1 drops to only 6%. We did not exceed the 2:1 ligand:S1 stochiometry in these

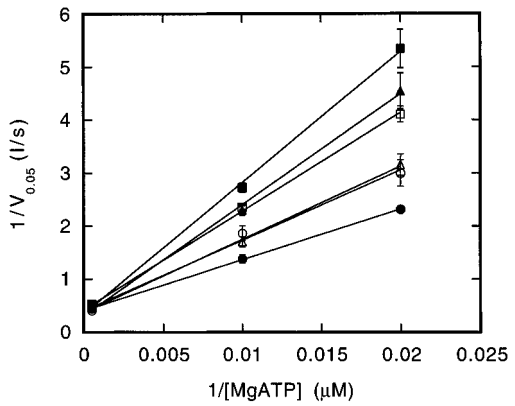

FIGURE 6: Double reciprocal plots of 1/(isotonic shortening velocity at 5% P_o) vs 1/[MgATP] for various concentrations of analogs. Conditions: 0 added analog (closed circles); 0.6 and 2.4 mM ATP-γCH$_3$ (open and closed triangles); 3 mM ATP-γSL (open circles); 1.5 and 3 mM AP$_5$A (open and closed squares). The least-squares linear fit in the absence of additional competitive ligand defines a K_m for $V_{0.05}$ of 234 μM MgATP. The slopes of the least-squares fits in the presence of a competing ligand were used to approximate a K_i for fiber velocity assuming classical competitive inhibition. Values are given in Table 1.

experiments in order to minimize any problems with possible nonligand contaminants. Hence, the lower fraction of S1 bound to AP$_5$A or ATP-γSL is able to account, at least in part, for the slower reactions seen with the analogs, enhancing our conclusion that the binding of the analogs produces a conformational change in S1 that indicates that the ligands are indeed binding to the S1 active site.

One additional control experiment is important to note. Ca^{2+}-ATPases were also observed under conditions where cross-linking was attempted in the presence of pPDM and AMP. For these experiments, the AMP employed was made by enzymatic degradation of an ADP stock by apyrase, following the protocols previously described to ensure uncontaminated ATP-γCH$_3$, ATP-γSL, and AP$_5$A. The Ca^{2+}-ATPases were not statistically different from those obtained in the presence of pPDM, without analog. Similar observations on a lack of an effect in the presence of AMP have been made previously (*26*). Any significant, residual ADP in our buffers would have instead yielded a reduced Ca^{2+}-ATPase. This provides additional confidence that our apyrase protocols are truly eliminating contaminating species. Of additional importance, this control shows that the other ligand-induced enhancements of pPDM cross-linking cannot simply be the result of nonspecific binding of the adenosine moieties to the myosin motor domain.

(4) Skinned Fiber Mechanics. The maximum shortening velocity (V_{max}) of skinned skeletal muscle fibers exhibits classical, Michaelis−Menten saturation kinetics with respect to [MgATP] (*36*, *37*). Nonhydrolyzable species that compete with ATP at the active site, such as ADP, PP$_i$, and AMPPNP, have been shown to function as classical competitive inhibitors of V_{max}. Furthermore, the K_i determined for this inhibition has been shown to be approximately equal to the dissociation constant for binding of the analogs to actoS1 (*38*−*41*). Figure 6 shows the effects of the nucleotide analogs on skinned fiber shortening velocity. As an approximation to V_{max}, fibers were allowed to shorten isotonically at 5% of isometric tension. Figure 6 gives double reciprocal plots of $1/V_{0.05}$ vs 1/[MgATP] in the absence of a competing ligand (solid circles) and for various concentrations (see figure legend) of ADP-γCH$_3$, AP$_5$A, and ATP-γSL. All data were well approximated by least-squares, linear fits ($r > 0.996$ for all fits). The least-squares linear fit to the velocity data defined a K_m for $V_{0.05}$ of 234 μM. This value is comparable to the 150−225 μM value we have previously suggested using rabbit psoas fibers for the K_m of fiber V_{max} at 10 °C (*36*, *38*). The common vertical intercept implies classical competitive inhibition, and the slopes of the least-squares fits for data in the presence of added nucleotide analog can be used to determine a value for K_i for each ligand. The values are given in Table 1. The important observation is that the values for K_i from our fiber velocity experiments differ at most by only about a factor of 2 from the values obtained for K_d to the actomyosin complex in myofibrils.

DISCUSSION

One of the many ways that ATP analogs have historically proved extremely valuable in the study of muscle mechanics has been in their ability to stabilize the contractile cycle in interesting, but otherwise transitory states. These states can then be analyzed by other biochemical or biophysical techniques. With myosin motor domain crystal structures now available, analog development may proceed in an even more focused fashion. The myosin crystal structures, augmented by comparison with related crystal structures from the G-protein superfamily, provide the basis for hypotheses as to specific domain movements which occur during the contractile cycle. Custom syntheses can then be undertaken to place moieties at crucial locations in order to test these hypotheses. This is the approach we have taken here.

We investigated the binding of a series of ATP analogs to S1 and to actomyosin in myofibrils and skinned fibers. The common thread running through all of the analogs was a desire to attach increasingly bulky groups to the γ-phosphate position of ATP. The sizes investigated ran from a single, small methyl group (ATP-γCH$_3$) to ADP, giving AP$_5$A as the analog. This allowed us to investigate the effects of modifications near the γ-phosphate on nucleotide binding and to suggest a previously unanticipated conformational change that takes place during ligand binding.

As is evident from Table 1, fluorescence competition experiments indicate that all of the ligands bind to S1 in solution. The binding of ATP-γSL and AP$_5$A to myosin are both clearly quite weak. This weak binding must be placed in the proper perspective, however. MgATP binds to myosin exceptionally tightly, with an affinity constant of approximately 10^{10} M^{-1} (for review, see ref *42*). Our data show that even a seemingly minor perturbation—addition of a small methyl group at the γ-phosphate position—reduces the binding affinity of the nucleotide to 40 μM, a change of 5−6 orders of magnitude. This analog provides a control for the effects of our addition of even bulkier groups. Indeed, it becomes surprising that AP$_5$A and ATP-γSL bind at all. However, the data of Table 1 indicate that the bulkier groups decrease the binding affinity to S1 by only an additional order of magnitude.

Three observations support the claim that the analogs bound to myosin at the nucleotide site in a fashion similar to other nucleotides, altering myosin conformation and being influenced by the binding of actin. First, the binding of actin to myosin reduces the affinity of nucleotides for myosin by

a factor of 20−100 for ADP (*43*), a factor of 10−100 for AMPPNP and PP_i (*41*), and a factor of 10^3−10^4 for ATP (reviewed in ref *44*). All of the ligands in the present studies had a similar behavior. The values for K_d in the actomyosin complex decreased by factors ranging from 5- to 20-fold when compared to the K_d for S1 alone and indicated that they must bind specifically to the active site in a conformation that senses the presence of actin. Second, all of the analogs potentiated the intrinsic, S1 tryptophan fluorescence, and third, all the analogs enhanced pPDM cross-linking of the reactive sulfhydryls. Both the change in tryptophan fluorescence and the cross-linking of the cysteines have been shown by a number of studies to monitor global changes in the structure of S1 due to specific binding of nucleotides to the active site. The sites of these actions, Trp-510 and the reactive cysteines, Cys 697 and Cys 707, are distant from the active site (amino acid numbering from the chicken sequence). All of the above observations could only have resulted from interactions between the analog and the protein that occur when the nucleotide analogs were interacting with specific groups at the active site.

A final set of experiments investigated competition in skinned fiber shortening velocity between ATP-γCH_3, ATP-γSL, and AP_5A and the physiological substrate. Linear double reciprocal plots of 1/shortening velocity vs 1/substrate concentration with consistent values for K_i have traditionally been taken as evidence that the ligand in question binds at the nucleotide site, competing with MgATP. We observe this behavior here and have been able to define a value K_i for the actomyosin interaction based upon shortening velocity. With regard to Table 1, the important observation is that the values for K_i we obtain from fiber shortening velocity as a function of [MgATP] and competing ligand are comparable to the K_d obtained from fluorescence-quenching competition experiments with myofibrilar actomyosin in solution. This has been previously observed for the more frequently employed competitive inhibitors of ATP: ADP, AMPPNP, and PP_i (*38*−*40*).

In summary, observations from several different experiments all support the hypothesis that the analogs bind to the active site of myosin. These include the facts that (1) they all compete with fluorescent nucleotides that are known to function at this site, (2) their apparent affinity is affected by the binding of actin, and (3) they induce alterations in the protein structure in a manner similar to native nucleotides at tryptophan and cysteine sites that are distant from the active site. The affinity of adenosine for the active site is much weaker than that of the analogs studied here. AMP does not promote cross-linking of the reactive sulfhydryls. These latter observations show that the three effects listed above must result from interaction of our analog phosphate moieties with the protein. The phosphate tube provides the only reasonable site for such an interaction. Thus, taking the data *in toto*, the simplest explanation for all of our observations is that these ligands are in fact binding to the active site via the phosphates and competing with MgATP. However, the exact nature of the interaction between the analogs and the protein must await determination of crystal structures of the myosin catalytic region complexed with the analogs.

Analog Purity. During the conduction of these experiments, trace contamination of our ligands by the much more tightly binding ATP and ADP was an overriding concern. As previously noted, all synthesized and purchased ligands were first purified by HPLC, additional enzymatic purification steps were subsequently employed, and the purified ligands were again checked using analytical HPLC. A number of observations, however, provided additional confidence that trace contaminants were not influencing our results. (1) In the tryptophan fluorescence experiments, AP_5A yielded the smallest increase in fluorescence and thus would be expected to be most sensitive to contamination. However, as evident in Figure 5, upon addition of AP_5A, fluorescence rose to the new, steady-state level without the single-turnover transient peak which would be seen in ATP-contaminated preparations. Likewise, any ADP contamination would result in a similar peak as it bound to S1 and was subsequently hydrolyzed to AMP by the apyrase present in the experimental buffers. (2) In the skinned fiber, velocity competition experiments, apyrase could not be included in the experimental buffers since it would have hydrolyzed the substrate. The experimental solutions did contain creatine phosphate and creatine kinase to buffer ATP levels interior to the fiber. Any ADP contamination of our ligands would be rapidly converted to ATP. Thus any ADP or ATP contamination of our ligands would result in an *increase* in the [MgATP] in the experimental solution, implying that we are actually *underestimating* the K_i of the competing species. (3) In the sulfhydryl cross-linking experiments, a 2:1 ligand:S1 ratio was used. Thus again, any trace ADP or ATP contamination would rapidly be trapped at the active site and thus make only a negligible contribution to the final decrease in the Ca^{2+}-ATPase activity induced by the ligand itself.

Relationship of AP_5A Binding to Other Skinned Fiber Studies. AP_5A is frequently used in skinned fiber studies in which mechanical perturbations as a function of ADP are of interest. AP_5A is added as a means of inhibiting endogenous myokinase activity in the fiber, thus preventing the synthesis of unwanted ATP. It is important to emphasize that our present observation that AP_5A itself actually binds to the actomyosin complex, and competes with other ligands, does not negate the conclusions of any fiber studies using AP_5A as a myokinase inhibitor of which we are aware. This is due to the fact that AP_5A concentrations are routinely kept at $<200\ \mu$M. At this level, the concentrations are sufficiently far below our measured dissociation constant of AP_5A from actomyosin to have only minimal effect on fiber mechanics in the presence of ADP.

Computer Molecular Docking of the Analogs. In order to better understand the interactions of the ligands investigated in the current studies, we have docked the ligands used in these studies into the *Dd* ADP·BeF_3 S1 X-ray crystal structure (*2*) using molecular modeling and computer graphics. Additional discussion of the docking protocols are provided in Methods. To date all X-ray structures of the myosin motor domain show a closed, tube-like protein structure surrounding the triphosphate portion of the substrate. The tube is formed by switch I, switch II, and the P-loop portions of myosin. One end of the tube opens into the open pocket in which the adenine and ribose rings are bound (approximately 13−15 Å across and 12 Å deep). The other end of the tube opens into the upper portion of the large cleft that splits the 50K domain into upper and lower subdomains (also termed the 50K cleft). For orientation, Figure 8 provides additional detail of this portion of S1. Other

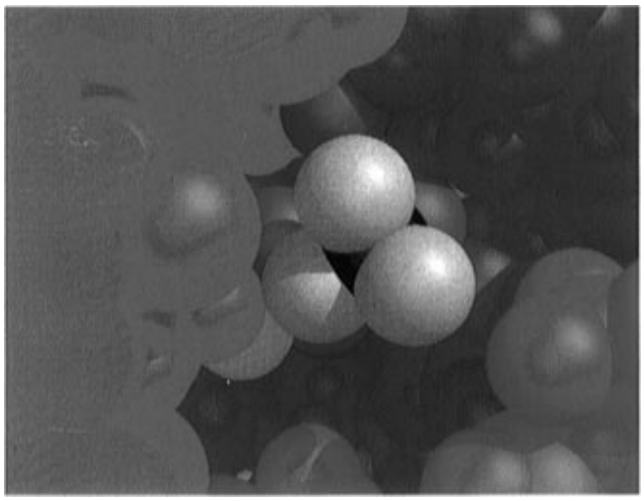

FIGURE 7: Conic view of ATP-γCH$_3$ docked in the P$_i$-tube from the *Dd* S1·ADP·BeF$_3$ X-ray crystal structure (Fisher et al., 1995). The view is looking up the 50K cleft into the P$_i$-tube. ADP·BeF$_3$ is shown in red. For the attached methyl group, the carbon is black and the hydrogens are white and protrude out of the P$_i$-tube into the 50K cleft. The metal is yellow. The P$_i$-tube is formed by switch I (green), switch II (magenta), and the P-loop (blue). Assuming a 1 Å van der Waals surface, there is no steric interference between the terminal methyl group and the protein.

excellent views are provided in Yount et al. (*7*). Figure 7 shows a conic surface of a computer docking of ATP-γCH$_3$ into the nucleotide binding site. The view is looking up the 50K cleft into the γ-phosphate end of the P$_i$-tube. The ATP portion of the analog is at the center in red, and the methyl group (carbon in black, hydrogens in white) protrudes into the 50K cleft opening.

The computer docking of ATP-γCH$_3$ was accomplished with no steric interference between the van der Waals surfaces of the terminal methyl group and the protein. However, a slight rotation of the side chain of Ser-456 was required, again producing no protein−protein interference. The necessity of only a minor side chain rotation, and the fact that the methyl group is small, would clearly tend to imply that binding of ATP-γCH$_3$, as well as ATP, could readily be postulated to occur via the triphosphate end of the ligands snaking through a closed P$_i$-tube. The 10^5-10^6-fold decrease in binding affinity of ATP-γCH$_3$ when compared to ATP would instead emphasize that maintenance of charge in the triphosphate portion is a major factor in the determination of the strength of binding.

In order to analyze the binding of other ligands we have examined, however, it is necessary to get a better description of the diameter of the P$_i$-tube. In reality, the protein boundary of the tube is rather irregular since it is composed of amino acid side chains that interact with the bound ligand. However, from the crystal structure, the narrowest passages are found between Asn-233 and Lys-185 (2.96 Å), Ser-237 and Ser-181 (3.44 Å), and Gly-182 and Ser-237 (4.07 Å). All of these distances include a 1 Å van der Waals radius around each residue. In other words, the P$_i$-tube is wide enough to let the triphosphate portion of ATP through without opening. Thus, the binding of ATP-γCH$_3$ introduces no compelling need to open the P$_i$-tube. However, an only slightly larger group will not be able to pass. This conclusion is also evident from the close packing of the P$_i$-tube to the triphosphate portion of the ligand as depicted in Figure 7.

The steric constraints would make it impossible for AP$_5$A to thread through the closed P$_i$-tube. Adenosine has an irregular structure, with the ribose ring roughly perpendicular to the plane of the adenine rings. The distance across the adenine ring from the H-8 to H-2 is 6.5 Å and from the N-3 to the amino hydrogen on C-6 is 5.3 Å. The distance across the ribose ring from the H-3′ to the 4′-ribose oxygen is 4.3 Å and from H-1′ to H-3′ is 5.1 Å. Between the adenine and ribose, the distance from OH-2′ to N-7 is N 6.5 Å; the distance from OH-3′ to the amino hydrogen on C-6 is 9.4 Å. After increasing all of these distances by 2 Å to account for the van der Waals surface, it is clear that these dimensions are incompatible with AP$_5$A binding through a closed P$_i$-tube. Furthermore, the P$_i$-tube is composed of a large number of hydrophilic side chains which coordinate to the negatively charged triphosphates. Thus the hydrophobic nature of adenosine introduces a further hindrance to passage through a closed P$_i$-tube.

Figure 8, however, dramatically makes the point that once AP$_5$A (red) has bound to S1, its presence is in fact compatible with the known X-ray crystal structure of the myosin motor domain. A stereo pair is shown. The adenine portion of the nucleotide pocket is at the upper left and the 50K cleft is at the center, bottom. The crystal structure P$_i$-tube is closed, surrounding three of the phosphates. The two additional phosphates thread through the P$_i$-tube, with the extra ribose and adenine rings fitting comfortably in the 50K cleft. The depicted sizes of the P$_i$-tube and the 50K cleft adenosine reemphasize our conclusion that AP$_5$A cannot bind through a closed P$_i$-tube.

AP$_5$A is a much longer molecule than ATP-γCH$_3$, reaching considerably further down into the 50K cleft. In order to dock AP$_5$A into the crystal structure without interference between the van der Waals surfaces of the docked ligand and the protein, we again found it necessary to rotate amino acid side chains. The most significant reorientations were at Phe-461 and Arg-232. Docking required a rotation of the phenyl ring of Phe-461. In the docked structure, the ring now lies roughly parallel to the plane of the adenine ring in the 50K cleft. In the crystal structure, Arg-232 projects out into the 50K cleft forming a 5.3 Å salt bridge with Glu-459. In order to dock AP$_5$A, it was necessary to break this salt bridge, rotating the side chain of Arg-232. van der Waals constraints also necessitated additional very minor side chain rotational movements around single bonds. These did not create any protein−protein interference. No other modifications of the crystal structure were required (e.g., backbone movements, bond length modifications, or nonrotational angular modifications), reemphasizing the significant gap the 50K cleft creates at the end of the P$_i$-tube. Nonetheless, from the figure, the important observation is that even with a closed P$_i$-tube, AP$_5$A can be very comfortably docked into the S1 nucleotide binding site. This brings to the fore our fundamental point: From the X-ray structure, it is clear that AP$_5$A can bind to S1 but cannot get into any bound S1 state without a prior opening of the P$_i$-tube.

Our experimental data also indicate that ATP-γSL binds to S1. With reference to Figure 1, the spin-label moiety in ATP-γSL is a five-membered ring. The ring is slightly puckered, with the four methyl groups projecting out of the "plane" of the ring. Looking edge-on into the plane of the ring from the nitroxide, the methyl groups project upwardly and downwardly. It is clear from the previous P$_i$-tube

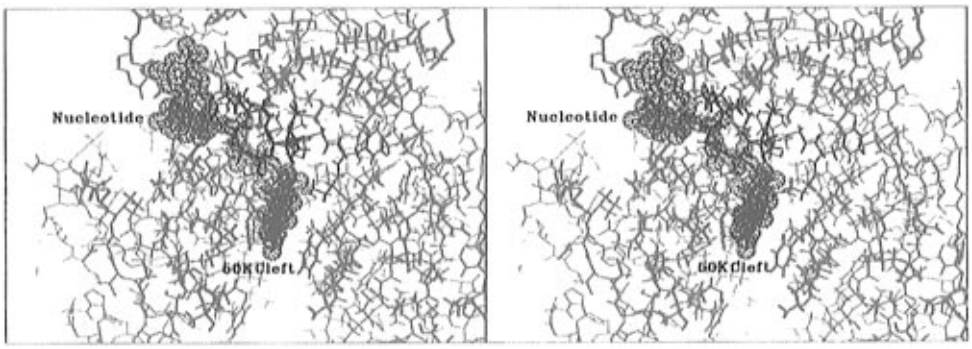

FIGURE 8: Stereo pair of AP_5A (red) docked at the nucleotide site in the *Dd* S1·ADP·BeF_3 X-ray crystal structure (cyan). The adenine portion of the nucleotide pocket is at the upper left; the 50 K cleft is at the center and bottom. The P_i-tube is closed. Also shown are the conserved portions of the P-loop (blue, amino acids 179−186 with increasing residue number as the backbone moves from right to left), switch I (orange, amino acids 233−238 with increasing residue number as the backbone moves into the plane of the figure), and switch II (magenta, amino acids 454−459 with increasing residue number as the backbone moves from top to bottom). As is evident, the extra adenosine moiety fits comfortably in the 50K cleft, with no steric interference assuming a 1 Å van der Waals surface. The extra adenosine moiety is too large to fit through the closed P_i-tube. The fact that our experimental evidence indicates that AP_5A does indeed bind to S1 implies that the P_i-tube must open during the contractile cycle. The docking protocols are discussed in Methods and Results.

dimensions that the requisite passage through the P_i-tube for the 7.9 Å × 6.3 Å (edge-on) spin-label moiety does not exist. As is the case with AP_5A, attempts at computer docking of ATP-γSL into the S1 structure reveal that the five-membered ring is located in the 50K cleft (structure not shown). However, the spacer group between ATP and the EPR ring is shorter than the spacer group between ATP and the extra adenosine moiety in AP_5A. Because of this, the EPR probe resides higher in the 50K cleft. Even after allowing for amino acid side chain rotations, it is not possible to dock ATP-γSL in the crystal structure without steric interference with either Arg-238, Ser-456, or Ser-181 (i.e., switch I, switch II, or the P-loop). This offers a possible explanation for our observation that ATP-γSL binds more weakly to S1 and is less effective at promoting pPDM cross-linking of SH-1 and SH-2 than is the significantly bulkier AP_5A.

We note that we are not the first to report the binding to myosin of an ATP analog with a bulky group at the γ-phosphate position. Sleep et al. (*12*) and Thirlwell et al. (*13*) suggested that caged-ATP (a substituted phenyl ring off of the γ-phosphate) binds to S1 and to actomyosin in fibers and in solution. As noted in Table 1, the binding affinity they measured was comparable to those we have measured for AP_5A and for ATP-γSL. Computer molecular docking studies indicated that caged ATP could indeed be docked into the S1 crystal structure with the phenyl ring in a position roughly equivalent to the docked spin ring from ATP-γSL (structures not shown). Since the caged ATP ring was planar, the protein−ligand steric interference present with ATP-γSL could be avoided, subject to noninterfering rotations of amino acid side chains. Combining caged ATP with the ligands studied here, we now have γ-phosphate-modified ATP analogs with a spectrum of sizes for the added moieties. Furthermore, the literature parameters for caged ATP are compatible with the observations reported in the present studies, reinforcing our conclusions.

Implications for the Interpretation of S1 Crystal Structures. The X-ray crystallographic solutions for nucleotide-free chicken S1 and nucleotide-bound *Dd* myosin motor domain all exhibit a tightly closed P_i-tube adjacent to a broad, very open nucleotide cleft. This cleft is 13−15 Å across at the surface of the protein. The base and ribose portions of ATP are seen to reside in this open pocket in the nucleotide-bound structures. *In vivo*, myosin-based motility is driven by ATP hydrolysis via domain movements in the vicinity of the nucleotide site, which are rectified and/or amplified in the remainder of the molecule. Since large-scale domain shifts would be required to close the adenosine pocket, there has been considerable interest in the possibility of isolating new myosin, X-ray crystallographic structures with a pocket that is more closed. Although this is clearly an important line of investigation, the arguments in its favor are most frequently predicated upon the view that, with such a new structure in hand, resolution of the open and closed ATP binding pocket conformations will have been obtained. To the contrary, the present studies—that require an opening of the P_i-tube—suggest that the nucleotide binding site is already at least partly closed in the extant X-ray structures. Thus one should also search for structures in which the nucleotide pocket is more open. Why do all the presently known structures show the P_i-tube closed? The most stable conformation could be closed with the open conformations being a transient event. The binding of ATP is sufficiently slow to accommodate such a scheme.

There is reason to believe that the closed form of the phosphate tube would become less stable in the absence of a bound ligand. In the structure of *Dd* S1 with bound ADP·BeF_3 there are seven hydrogen bonds between the residues that form switch I and the Mg·nucleotide complex and four additional hydrogen bonds via crystal waters. There are none between switch I and the other side of the phosphate tube (ref *2*; Figure 6). In the ADP·VO_4 structure, there are nine hydrogen bonds between the residues that form switch I and the Mg·nucleotide complex and only 1 hydrogen bond (Arg-238 to Glu-459) to the other side of the P_i-tube (ref *3*; Figure 11). Thus the presence of a bound ligand would be expected to exert a significant stabilizing influence on the closed P_i-tube.

Is Myosin a "Trap Door" Enzyme? We have shown that ATP analogs with large moieties at the γ-phosphate position that preclude passage through a closed P_i-tube are still capable of binding to S1 and to actomyosin. The affinity of the analogs does not depend strongly on the size of the group and is of the same order of magnitude as observed for AMPPNP and for PP_i (*40*, *41*). The latter two species, along with ATP-γCH_3, would appear clearly capable of binding through a closed P_i-tube. Together, these data show that the opening of the P_i-tube is not an isolated, rare event

but that it occurs sufficiently often to provide little barrier to the binding of the more bulky analogs. This conclusion suggests that binding of ATP through an open tube, rather than threading of the phosphates through the tube, may be a fundamental part of the chemomechanical cycle. Thus, we are now able to propose a new mechanism by which substrate binding occurs.

As previously noted, the γ-phosphate position is clearly visible looking up the large cleft in the 50K domain into the P_i-tube (*7*). Following hydrolysis on the myosin head, P_i is released prior to ADP (reviewed in ref *42*). These observations, coupled with the fact that the γ-phosphate is more deeply buried at the nucleotide site than the ADP portion of the substrate (see Figures 7 and 8), have led to the hypothesis that myosin is a "back door" enzyme. By this it is meant that since the "front door" of the P_i-tube is blocked by ADP following the hydrolysis step, P_i can only be released via the back door into the 50K cleft (*7*).

It is important to note that our present observations are not necessarily in conflict with a back door mechanism for phosphate release. However, they do now suggest a more complex, trap door, mechanism for MgATP binding to myosin. In such a scheme, initial nucleotide binding does not occur via a threading of the triphosphate portion of ATP down through the closed, P_i-tube seen in the crystal structure. Instead, initial MgATP binding occurs to a myosin conformation in which switch 1 has pulled back and the P_i-tube is open as in the ncd and kinesin X-ray crystallographic structures. When thermal forces place the triphosphates in the correct spatial location to maximize protein−metal−ligand coordination, the trap door (i.e., switch 1) swings shut, closing the P_i-tube. Hydrolysis follows, and the now trapped hero(ine) of our melodrama, P_i, has no way to escape except down the P_i-tube into the 50K cleft and out the back door. The loss of ligand−protein coordination following P_i and/or ADP release allows the trap door to be reset into the open, empty position, and another hapless ligand can now be snared.

The concept that substrates initially bind to a protein site with an open configuration, and that this open configuration subsequently closes, is a frequently observed phenomenon in structural biology. An open hexokinase binding pocket is seen to close upon the binding of glucose and P_i (*45*). Similar closures are seen in citrate synthase (*46*), alcohol dehydrogenase (*47*), and adenylate kinase (*48*). Thus, the opening of the P_i-tube and subsequent closure for the ATP hydrolysis step described above do not represent any really new or radical concept in the physical chemistry of proteins. It is simply the application of these ideas to a new protein structure.

ACKNOWLEDGMENT

We acknowledge the invaluable assistance provided by members of the laboratory of R. Yount: J. Grammer for help with the pPDM cross-linking experiments; D. Lawson and R. Yount for numerous valuable discussions on both computer molecular modeling and the X-ray crystallographic structure of the P_i-tube. Synthesized compounds were analyzed by the UCSF Mass Spectroscopy facilities, Al Burlingame, Director, supported by NIH Grant NCRR BRTP RR01614. Computer graphics support was provided by the UCSF Computer Graphics Laboratory, supported by NIH Grant P41-RR01081. We thank T. Pham and Wei Wang for technicial assistance and R. Fletterick, J. Kull, and E. Sablin for providing the X-ray coordinates to kinesin and ncd prior to publication.

REFERENCES

1. Rayment, I., Rypniewski, W. R., Schmidt-Base, K., Smith, R., Tomchick, D. R., Benning, M. M., Winkelmann, D. A., Wesenberg, G., and Holden, H. M. (1993) *Science 261*, 50−57.
2. Fischer, A. J., Smith, C. A., Thoden, J., Smith, R., Sutoh, K., Holden, H. M., and Rayment, I. (1995) *Biochemistry 34*, 8960−8972.
3. Smith, C. A., and Rayment, I. (1996) *Biochemistry 35*, 5404−5417.
4. Kull, F. J., Sablin, E. P., Lau, R., Fletterick, R. J., and Vale, R. D. (1996) *Nature 380*, 550−555.
5. Sablin, E. P., Kull, F. J., Cooke, R., Vale, R. D., and Fletterick, R. J. (1996) *Nature 380*, 555−559.
6. Vale, R. D. (1996) *J. Cell Biol. 135*, 291−302.
7. Yount, R. G., Lawson, D., and Rayment, I. (1995) *Biophys. J. 68*, 44s−49s.
8. Walker, J. E., Saraste, M., Runswick, M. J., and Gay, N. J. (1982) *EMBO J. 1*, 945−951.
9. Bourne, H. R., Sanders, D. A., and McCormick, F. (1991) *Nature 349*, 117−127.
10. Coleman, D. E., Berghuis, A. M., Lee, E., Linder, M. E., Gilman, A. G., and Sprang, S. R. (1994) *Science 265*, 1405−1412.
11. Jeldgaard, M. K., Nissen, P., Thirup, S., and Nyborg, J. (1993) *Structure 1*, 35−50.
12. Sleep, J., Herrmann, C., Barman, T., and Travers, F. (1994) *Biochemistry 33*, 6038−6042.
13. Thirlwell, H., Sleep, J. A., and Ferenczi, M. A. (1995) *J. Muscle Res. Cell Motil. 16*, 131−137.
14. Eckstein, F., Bruns, W., and Parmeggiani, A. (1975) *Biochemistry 14*, 5225−5232.
15. Hideg, K., Hankovszky, H. O., Lex, L., and Kulcsar, Gy. (1980) *Synthesis*, 911−916.
16. Margossian, S. S., and S. Lowey (1982) *Methods Enzymol. 85*, 55−71.
17. Franks-Skiba, K., Hwang, T., and Cooke, R. (1994) *Biochemistry 33*, 12720−12728.
18. McCubbin, W. D., Willick, G. E., and Kay, C. M. (1973) *Biochem. Biophys. Res. Commun. 50*, 926−933.
19. Onishi, H., Ohtsuka, E., Ikehara, M., and Tonomura, Y. (1973) *J. Biochem. 74*, 435−450.
20. Ando, T., Duke, J. A., Tonomura, Y., and Morales, M. F. (1982) *Biochem. Biophys. Res. Commun. 109*, 1−6.
21. Rosenfeld, S. S., and Taylor, E. W. (1984) *J. Biol. Chem. 259*, 11908−11919.
22. Pate, E., Franks, K., White, H. D., and Cooke, R. (1993) *J. Biol. Chem. 268*, 10046−10053.
23. Traverso-Cori, A., Traverso, S., and Reyes, H. (1970) *Arch. Biochem. Biophys. 137*, 133−142.
24. Bradford, M. M. (1976) *Anal. Biochem. 72*, 248−254.
25. Cooke, R., and Franks, K. (1980) *Biochemistry 19*, 2265−2269.
26. Wells, J. A., and Yount, R. (1982) *Methods Enzymol. 85*, 93−116.
27. Shimizu, T., and Furusawa, K. (1986) *Biochemistry 25*, 5787−5792.
28. Cooke, R., Franks, K., Luciani, G., and Pate, E. (1988) *J. Physiol. 395*, 77−97.
29. Pate, E., Nakamaye, K. L., Franks-Skiba,K., Yount, R. G., and Cooke, R. (1991) *Biophys. J. 59*, 598−605.
30. Pate, E., Wilson, G., Bhimani, M., and Cooke, R. (1994) *Biophys. J. 66*, 1554−1562.
31. Park, S., Ajtai, K., and Burghardt, T. P. (1996) *Biochim. Biophys. Acta 1296*, 1−4.
32. Sellers, J. R., and Goodson, H. V. (1995) *Protein Profile 2*, 1323−1423.
33. Goody, R. S., and Hofmann, W. (1980) *J. Muscle Res. Cell Motil. 1*, 101−115.

34. Reisler, E., Burke, M., Himmelfarb, S., and Harrington, W. F. (1974) *Biochemistry 13*, 3837−3840.
35. Burke, M., and Reisler, E. (1977) *Biochemistry 16*, 5559−5563.
36. Cooke, R., and Bialek, W. (1979) *Biophys. J. 28*, 241−258.
37. Ferenczi, M. A., Goldman, Y. E., and Simmons, R. M. (1984) *J. Physiol. 350*, 519−543.
38. Cooke, R., and Pate, E. (1985) *Biophys. J. 48*, 789−798.
39. Glyn, H., and Sleep, J. (1985) *J. Physiol. 365*, 259−276.
40. Pate, E., and Cooke, R. (1985) *Biophys. J. 48*, 773−780.
41. Biosca, J. A., Greene, L. E., and Eisenberg, E. (1986) *J. Biol. Chem. 261*, 9793−9800.
42. Taylor, E. W. (1979) *CRC Crit. Rev. Biochem. 6*, 103−164.
43. Greene, L. E., and Eisenberg, E. (1980) *J. Biol. Chem. 255*, 543−548.
44. Sleep, J. A., and Smith, S. J. (1981) *Curr. Top. Bioenerg. 11*, 239−287.
45. Steck, T. L., Weinstein, R. S., Straus, J. H., and Wallach, D. F. H. (1970) *Science 168*, 255−257.
46. Steck, T. L., and Yu, J. (1973) *J. Supramol. Struct. 1*, 220−232.
47. Carpenter, G. (1987) *Annu. Rev. Biochem. 56*, 881−914.
48. Schulz, G. E., Mueller, C. W., and Diederichs, K. (1990) *J. Mol. Biol. 213*, 627−630.

BI970996Z